

CENA FM Calibration Report
Issue 1 Revision 0

Martin Wieser
Swedish Institute of Space Physics, IRF, Kiruna, Sweden

January 24, 2010

Document Revision History

Issue	Revision	Date	Remarks
Draft 1	-	26 June 2009	First draft version
Draft 2	-	8 October 2009	Second draft version
1	pre1	10 January 2010	Initial version
1	pre2	15 January 2010	Revision by YF
1	0	24 January 2010	Initial release

IMPORTANT NOTE: WITH RELEASE OF THIS VERSION OF THIS DOCUMENT, ANY EARLIER VERSION OF THIS DOCUMENT BECOMES INVALID AND **MUST NOT** BE USED ANYMORE FOR DATA PROCESSING.

THIS DOCUMENT CONTAINS IN VARIOUS PLACES NOTES MARKED LIKE **ToDo: To be updated**. THESE NOTES INDICATE TOPICS THAT ARE ALREADY NOW KNOWN TO BE UPDATED IN A FUTURE VERSION OF THIS REPORT. CARE SHOULD BE USED WHEN PROCESSING DATA RELATED TO THESE TOPICS - IT IS IMPORTANT THAT THE LIMITATIONS LEADING TO THE NOTE ARE UNDERSTOOD TO AVOID ERRORS.

Contents

1	The instrument	5
1.1	Coordinate systems	5
1.2	Zero-based numbering	5
2	Electrical interface	7
2.1	Conversion functions	7
2.2	Monitors	7
2.3	References	7
3	Sensor properties	9
3.1	Angular pixels	9
3.2	Open aperture	10
3.3	Center energy and energy resolution	10
3.4	Accumulation time	11
3.5	Geometric factor	11
3.5.1	Definitions	11
3.5.2	Estimation of geometric factor for hydrogen	12
3.6	How mass information is obtained	14
3.6.1	Mass calculation and binning	14
3.6.2	Convert mass bin to atomic mass number	15
	Abbreviations	16

Chapter 1

The instrument

1.1 Coordinate systems

Figure 1.1 depicts the relation of the coordinate systems used in this calibration report.

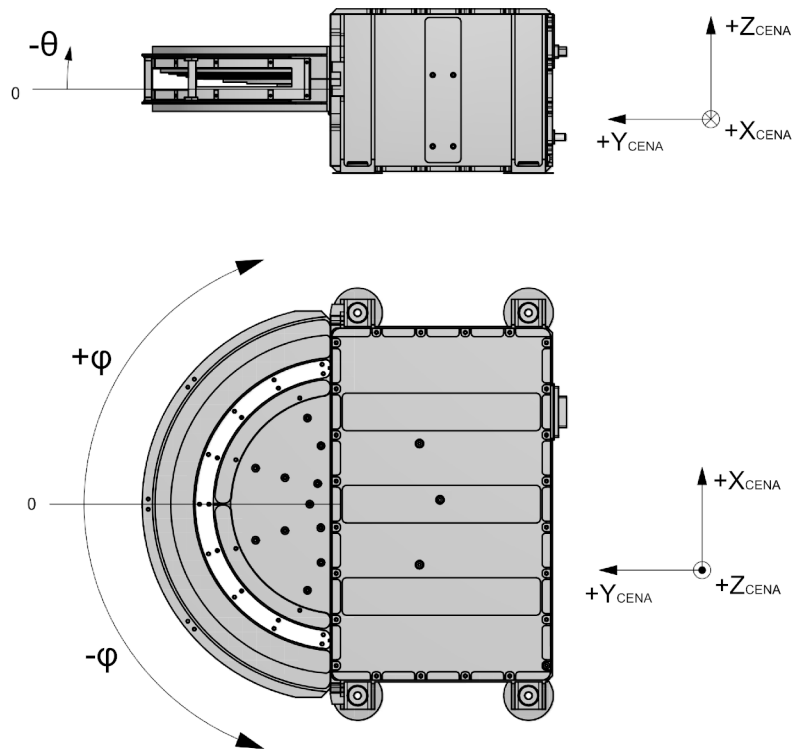


Figure 1.1: CENA angular coordinate system

1.2 Zero-based numbering

Zero based numbering is used throughout this document for sectors, mass bins, energy steps and so on; e.g. the seven azimuthal sectors are numbered $s_0, s_1, s_2, s_3, s_4, s_5, s_6$.

IMPORTANT NOTE: IN EARLY VERSIONS OF THE INSTRUMENT DESCRIPTION, IN SOME PLACES IN THE SICD AND IN THE TCTM DOCUMENTATION OF THE DPU A ONE-BASED NUMBERING WAS USED FOR SPECIFIC CASES. **ALWAYS CHECK BEFORE USE!**

Chapter 2

Electrical interface

2.1 Conversion functions

CENA contains internally five separately controllable high voltages plus two temperature monitors. Voltages are controlled by references and measured by monitors. There are two sets of conversion functions for high voltages: a) convert a digital reference value to a predicted voltage, b) convert a digital monitor value to a measured voltage. Both conversions use function of the type

$$y = p (ax^2 + bx + c) \tag{2.1}$$

where:

- a, b and c are tabulated coefficients,
- x is the digital monitor (ADC value; 12 bit unsigned integer) or digital reference (DAC value; 12 bit unsigned integer) and,
- y is the corresponding value in physical units.
- p is the polarity of the high voltage

2.2 Monitors

Conversion coefficients for digital monitor values are given in Table2.1. Note that x is always a positive value. Some high voltages are nevative voltages in the sensor, and some exist in both polarities; the polarity p indicates which case is applicable.

2.3 References

Table 2.2 shows coefficients to convert digital reference values to expected physical units. These values should be used if the monitor readings can not be used for any reason. Note that in order for the predicted voltage to be correct, the expression in parenthesis in Equation 2.1 (prior multiplication with the polarity p) must be positive. If the expression in parenthesis in Equation 2.1 is negative, then the predicted voltages are invalid.

Table 2.1: Coefficients to convert digital monitor values to physical units

Monitor name	<i>a</i>	<i>b</i>	<i>c</i>	Physical unit for <i>y</i>	Polarity <i>p</i>
HV_Ref (=HV_main)	0.0	1.22070 ¹⁾	0.0	Volts	+
HV_StartMCP	0.0	1.22070 ¹⁾	0.0	Volts	-
HV_StopMCP	0.0	1.22070 ¹⁾	0.0	Volts	-
HV_TOF ²⁾	0.0	0.000122070 ³⁾	0.0	Volts	+
HV_Def	0.0	1.22070 ¹⁾	0.0	Volts	+
SV_WAVE1 (any level)	0.0	1.22070 ¹⁾	0.0	Volts	-
SV_WAVE2A (any level)	0.0	1.22070 ¹⁾	0.0	Volts	-
SV_WAVE2B (any level)	0.0	1.22070 ¹⁾	0.0	Volts	-
SV_LENS (any level)	0.0	1.22070 ¹⁾	0.0	Volts	-
Temp_HVPS	0.0	0.196888	-273.16	degC	
Temp_IFE	0.0	0.196888	-273.16	degC	

Notes:

- 1) The exact value is equal to 5000.0 / 4096.0
- 2) The monitorline for HV_TOF is not connected to any HV and shows the value of HV_TOF reference voltage
- 3) The exact value is equal to 5.0 / 4096.0
- 4) The exact value is equal to 5000.0 / (4096.0 * 6.2)

Table 2.2: Coefficients to convert digital references to predicted voltages

Reference name	<i>a</i>	<i>b</i>	<i>c</i>	Physical unit for <i>y</i>	Polarity <i>p</i>
HV_Ref (=HV_main)	0.0	22.33	243.9	Volts	+/-
HV_StartMCP	0.0	14.80	-267.2	Volts	-
HV_StopMCP	0.0	14.86	95.3	Volts	-
HV_TOF ¹⁾	-	-	-		
HV_Def	0.0	1.299	-203.3	Volts	+

Notes:

- 1) This reference does not drive a HV and is connected directly to HV_TOF monitor

Chapter 3

Sensor properties

3.1 Angular pixels

For each angular pixel, the angular response to the actual flux has been calibrated on ground. The effective area where the response is high enough is called pixel. The shape of the response $S_n(\varphi, \theta)$ for the angular pixel of index n for correlated events (obtained in mass accumulation mode) are of the form

$$S_n = e^{-\left(\frac{(\varphi - \varphi_{c,n})^2}{2\sigma_n^2} + \frac{(\theta - \theta_{c,n})^2}{2\zeta_n^2}\right)} \quad (3.1)$$

with φ the viewing angle in azimuth direction, $\varphi_{c,n}$ the azimuth center for the pixel n , and $\sigma_n \approx FWHM_{\varphi,n}/2.35$ the azimuthal width θ the viewing angle in elevation direction, $\theta_{c,n}$ the center and $\zeta_n \approx FWHM_{\theta,n}/2.35$ the width in elevation. Equations 3.2 to 3.5 and Table 3.4 give a parametrization for these constants. The values are valid for 1keV hydrogen.

$$\varphi_{c,n} = -19.06 \cdot n + 57.19 \quad [\text{deg}] \quad (3.2)$$

$$FWHM_{\varphi,n} = 45.0 \quad [\text{deg}] \quad (3.3)$$

$$\theta_{c,n} = -6.05 \quad [\text{deg}] \quad (3.4)$$

$$FWHM_{\theta,n} = 6.44 \quad [\text{deg}] \quad (3.5)$$

It may be sometimes useful for scientific data analysis to add sectors 2, 3 and 4 up to form one big angular pixel (labeled 2-3-4). In this case the following values apply in azimuth direction:

$$\varphi_{c,2-3-4} = 0.0 \quad [\text{deg}] \quad (3.6)$$

$$FWHM_{\varphi,2-3-4} = 60.0 \quad [\text{deg}] \quad (3.7)$$

Often simplified rectangular sector shapes are useful. Their solid angle coverage is for the given relatively small pixels well approximated by $\Delta\Omega_n$:

$$\Delta\Omega_n \approx FWHM_{\varphi,n} \cdot FWHM_{\theta,n} \quad [\text{sr}] \quad (3.8)$$

3.2 Open aperture

The extent of the open aperture ΔA is geometrically defined by the colimator and approximately evaluated as $\Delta A \approx \sin(\theta_{c,n}) \cdot r_{CS} \cdot w_{CS}$, with $\theta_{c,n}$ from Equation 3.4, r_{CS} the radial extent of the conversion surface and w_{CS} the effective width of the aperture determined from calibration data obtained by translation scan. For simplicity, the size of the open aperture is assumed to be constant for all sectors. Any variations will be absorbed in one of the factors used to describe the of the sensitivity of each pixel (or sector¹), s_n , to be described later (see Equation 3.16).

$$\Delta A = 1.09 \text{ cm}^2 \tag{3.9}$$

3.3 Center energy and energy resolution

There are in total 16 different “energy settings” . Each “energy setting” defines the energy band of the measured ENAs, and we refer to the center energy of the energy band for the energy setting i as E_i hereafter. CENA has 3 energy sweep tables, and each of table consists of 8 energy settings, selected from the 16 that are available. Table 3.1 shows the central energy of ENAs of the selected energy table and the energy bin.(Energy tables are for historical reasons also called SV-tables, and the number of the active energy table is called SV-index). For Tables 2 and 3, the data obtained from energy bin $b = 0$ should not be used for science data analysis because these energy bins are contaminated by other energy settings due to a limited HV sweeping speed.

Table 3.1 shows the preliminary values of the bin energy centers for H^0 . For heavier species, the energy bin center center shifts to higher energies. Additionally, limited high voltage sweeping speed in the wave system results in an estimated error of E_i of about 15% at energies below 200 eV. **ToDo:** Update table 3.1 with higher accuracy values for hydrogen and for other species.

Table 3.1: Table to convert the energy bin b and SV table number to the center energies for E_i (H^0) . For a future reference, the index of the energy setting, i , is also shown. *) The data from the energy bin 0 should not be used for scientific analysis (see text).

Energy bin b	Table 1		Table 2		Table 3	
	E_i [eV]	i	E_i [eV]	i	E_i [eV]	i
0	193	8	652*	11	3300*	15
1	129	7	435	10	2200	14
2	86	6	290	9	1467	13
3	57	5	193	8	978	12
4	38	4	129	7	652	11
5	25	3	86	6	435	10
6	17	2	57	5	290	9
7	11	1	38	4	193	8

Energy resolution of the wave system is $\frac{\Delta E_i}{E_i} \approx 1$. A first approximation for the energy pass band $E_{PASS,H}$ for hydrogen is a skewed triangle with the peak at E_i and with these half maximum points:

$$E_{PASS,H} \approx 0.6E_i..1.6E_i \tag{3.10}$$

The approximation is good for all center energies E_i . This means that the energy bins overlap as the energy bin centers are spaced by a factor of 1.5. This needs to be considered when integrating physical flux over the energy steps. **ToDo:** Generate fit functions in energy space to model the shape of the passband more accurately.

¹The terms *pixel* and *sector* are synonyms and mean the same thing in this document

3.4 Accumulation time

Accumulation time for one measurement cycle is 4 seconds. Multiples of 4 seconds are also possible in principle, but this was never used during the mission. The sensor changes energy settings every $t_{SLOT} = 31.25$ ms. This results in a total available time of 500 ms for each energy bin in a 4 second accumulation interval. Dead time t_D from energy sampling is constant and 25% of t_{SLOT} . During the dead time the sensor does not record any data. For all calculations, measurement time Δt for each energy step in a 4 second accumulation interval is

$$\Delta t = \frac{4s}{8} \cdot \left(1 - \frac{t_D}{t_{SLOT}}\right) = 375\text{ms} \quad (3.11)$$

3.5 Geometric factor

3.5.1 Definitions

Differential number flux $J_{n,i,m}$ [#/(cm² sr eV s)] seen by each sector n and energy step i (with center energy E_i [eV]) and species m is given by

$$J_{n,i,m} = \frac{C_{n,i,m}}{\tilde{G}_{n,i}^m \cdot \Delta E_i \cdot \Delta t} \quad (3.12)$$

with $C_{n,i,m}$ [#] the number of counts accumulated during the accumulation time Δt [s]. The combined geometric factor $\tilde{G}_{n,i}^m \cdot \Delta E_i$ [cm² sr eV] for each sector n and energy step i is approximated as

$$\tilde{G}_{n,i}^m \cdot \Delta E_i = k_{n,i,m} \cdot A \cdot \Delta \Omega_n \cdot \left(\frac{\Delta E_i}{E_i}\right) \cdot E_i \quad (3.13)$$

with $\Delta E_i/E_i$ [eV/eV] the energy resolution of the wave system, $k_{n,i,m}$ including all efficiencies, A the ideal open area, $\Delta \Omega_n$ the angular pixel size. Note that the open area must depend on the sector n . However, this sector dependence cannot be known separately in practice, what we can know is its product with the other efficiencies. Therefore, the sector dependence of the open area is merged to $k_{n,i,m}$.

Introducing the parameter $G_{n,i}^m$,

$$G_{n,i}^m = k_{n,i,m} \cdot A \cdot \Delta \Omega_n \cdot \left(\frac{\Delta E_i}{E_i}\right) \quad (3.14)$$

3.15 can be rewritten as

$$J_{n,i,m} = \frac{C_{n,i,m}}{G_{n,i}^m \cdot E_i \cdot \Delta t} \quad (3.15)$$

The coefficient $k_{n,i,m}$ from Equation 3.14 can be split into energy and species dependent component $e_{i,m}$, sector dependent component s_n and an energy and sector independent component σ :

$$k_{n,i,m} = \sigma \cdot e_{i,m} \cdot s_n \quad (3.16)$$

The sector dependent component s_n will be tabulated in the later sections, and the other two factors are calculated by

$$e_{i,m} = \eta_{i,m}^+ \quad (3.17)$$

$$\sigma = T_1 \cdot T_2 \cdot r_{CS} \cdot \eta_{START} \cdot \eta_{MCP} \cdot \eta_{TOF} \cdot \left(1 - \frac{t_D}{t_{SLOT}}\right) \quad (3.18)$$

The components are listed in Table 3.2.

Table 3.2: Efficiency factor components in Equations 3.16 to 3.18.

Item	Symbol	Defining factor
First grid, transparency	T_1	Geometrically defined
Second grid, transparency	T_2	Geometrically defined
Collection efficiency of wave system from CS	r_{CS}	CS, ion optics, weakly energy dependent
positive ion yield at CS	$\eta_{i,m}^+$	Energy and species dependent
Start surface electron yield	η_{START}	Due to post acceleration
Start MCP efficiency	η_{MCP}	MCP bias and geometry
TOF efficiency	η_{TOF}	correlated rate/ start rate, from inflight data
Sector sensitivity	s_n	Instrument geometry, preamplifier settings

For some factors in Equation 3.18 the species independence is an approximation only which might partially be validated from flight data in each case: η_{START} , r_{CS} and η_{TOF} .

3.5.2 Estimation of geometric factor for hydrogen

Species and energy dependent efficiencies for hydrogen atoms in Equation 3.16 are shown in Tables 3.3. Here we introduce the reference geometric factor for hydrogen, G_i^H as written by

$$G_{n,i}^H = \sigma \cdot A \cdot e_{i,H} \cdot \left(\frac{\Delta E_i}{E_i} \right) \cdot [s_n \cdot \Delta \Omega_n] = G_i^H \cdot [s_n \cdot \Delta \Omega_n] \quad (3.19)$$

Now the G_i^H is independent of the sector n . The complete g-factor $G_{n,i}^H$ can be obtained by multiplying $s_n s_n$ and $\Delta \Omega_n$, which are in Table 3.4 and Equation 3.8).

Table 3.3: Efficiency factors for H^0

Symbol	Value valid for H	Comment
T_1	0.88	Geometrically defined
T_2	0.88	Geometrically defined
r_{CS}	0.7	Weak dependence on energy, to be investigated
$\eta_{i,H}^+$	$0.005 + 0.05 \cdot \frac{E_i}{E_0}$	From: Wieser et al, 2002. $E_0 = 1000\text{eV}$
η_{START}	1.0	post acceleration of ions with 2.4kV
η_{MCP}	0.15	2.1kV start MCP bias
η_{TOF}	0.045	Uncorrelated start to correlated rate, from flight data

Table 3.4: Relative for sector sensitivities s_n . The line 2 – 3 – 4 is valid for a combined center pixel made out of sectors 2 to 4.

Sector n	s_n
0	0.525
1	0.188
2	0.443
3	0.165
4	0.613
5	0.270
6	0.285
2-3-4	1.000

The energy dependence of the reference geometric factor G_i^H is tabulated in Table 3.5. This is valid for coincidence events from mass accumulation mode. Only mass bins $m^+ < 63$ (see Equation 3.28) have to be used. $G_{n,i}^H$ includes all efficiencies

Flux for a specific sector and energy bin is calculated using Equations 3.15 and 3.19. Again note that the $\Delta t = 375$ ms should be used for Equation 3.15.

Table 3.5: Energy dependent geometric factor G_i^H for H^0 . **The values shown have a uncertainty of a factor of 3 (1σ).** Equation 3.19 shows how to calculate the GF for a single sector. As examples, the geometric factor for the pixels $G_{2-3-4,i}^H$ and $G_{3,i}^H$ are shown.

Energy bin center for H^0 [eV]	Energy setting i	G_i^H [$cm^2 eV/eV$]	$G_{2-3-4,i}^H$ [$cm^2 sr eV/eV$]	$G_{3,i}^H$ [$cm^2 sr eV/eV$]
11	1	n/a		
17	2	n/a		
25	3	n/a		
38	4	$2.1 \cdot 10^{-5}$	$2.3 \cdot 10^{-6}$	$2.7 \cdot 10^{-7}$
57	5	$2.4 \cdot 10^{-5}$	$2.6 \cdot 10^{-6}$	$3.1 \cdot 10^{-7}$
86	6	$2.8 \cdot 10^{-5}$	$3.1 \cdot 10^{-6}$	$3.7 \cdot 10^{-7}$
129	7	$3.5 \cdot 10^{-5}$	$3.8 \cdot 10^{-6}$	$4.5 \cdot 10^{-7}$
193	8	$4.5 \cdot 10^{-5}$	$4.8 \cdot 10^{-6}$	$5.8 \cdot 10^{-7}$
290	9	$6.0 \cdot 10^{-5}$	$6.4 \cdot 10^{-6}$	$7.7 \cdot 10^{-7}$
435	10	$8.2 \cdot 10^{-5}$	$8.8 \cdot 10^{-6}$	$1.1 \cdot 10^{-6}$
652	11	$1.2 \cdot 10^{-4}$	$1.2 \cdot 10^{-5}$	$1.5 \cdot 10^{-6}$
978	12	n/a		
1467	13	n/a		
2200	14	n/a		
3300	15	n/a		

3.6 How mass information is obtained

3.6.1 Mass calculation and binning

Each valid TOF event consists of

1. Start ring number
2. Start sector number
3. Stop Plate number
4. Time of flight

Mass m of a particle is calculated onboard by evaluating

$$E_p + U_{TOF} \cdot e = \frac{1}{2} m m_p v^2 \quad (3.20)$$

with E_p [eV] the energy of the particle, U_{TOF} [V] the postacceleration that the particle experiences when it reaches the TOF section, e the elementary charge, m_p the proton mass, v the velocity of the particle in the TOF section, and m the mass in amu. The calculation does not include any energy loss at various reflecting surfaces for reasons given below. Using $v = \frac{s}{t}$, where s the pathlength in the TOF section and t the measured TOF and $U_P = \frac{E_p}{e}$, \sqrt{m} is obtained by

$$\sqrt{m} = \sqrt{\frac{2e}{m_p}} \cdot \sqrt{(U_{TOF} + U_P) e \cdot t \cdot s^{-1}} \quad (3.21)$$

Note that the pathlength s depends on the ring, sector and plate index.

We introduce parameters LT , TT and SVE (which are tables written in onboard memory) as ,

$$LT = \frac{2^{16}}{1000 s} \quad (3.22)$$

$$TT = \frac{t}{2 \cdot 10^{-6}} \cdot 1024 \quad (3.23)$$

$$SVE = 12 \cdot \sqrt{U_{TOF} + U_P} \quad (3.24)$$

where LT proportional to the inverse of the TOF path length, TT proportional to the time of flight and SVE a proportional to the energy of the particle in the TOF section depending on energy step. As an intermediate step, the mass index m^* is defined and calculated on the DPU as :

$$m^* = k \cdot SVE_{E-index} \cdot TT_{E-index,TOF} \cdot LT_{E-index,ring,sector,plate} \quad (3.25)$$

Indiezes indicate the lookup table index numbers: $E-index$ is the index corresponding to the selected center energy, TOF is the raw TOF value as reported in the TOF event, $ring, sector, plate$ are the start ring, start sector and stop plate numbers associated with the TOF event.

The scaling constant k is made such that $\sqrt{m} = \frac{m^*}{\sqrt{512}}$, assuming the energy loss on the start surface is 0. The final mass group M in which the event is accumulated in the DPU is obtained by

$$m^+ = \begin{cases} m^* \leq 63 & : m^* \\ m^* > 63 \wedge m^* < 255 & : \text{round}\left(\frac{m^*+1}{3}\right) + 42 \\ otherwise & : 127 \end{cases} \quad (3.26)$$

$$M = \text{floor}\left(\frac{m^+}{\text{floor}\left(\frac{128}{n_M}\right)}\right) \quad (3.27)$$

with n_M the number of mass bins selected on the DPU². Equation 3.26 is implemented using the lookup table MT . The algorithm implemented on the DPU is described below.

²In older documentation $n(M)$ is used to indicate the number of mass bins, or generally $n(X)$ to indicate the number of bins used for property X.

- R1 symbolizes a 32 bit register;
- TT, LT, SVE, SVM are arrays of constants
- Values of TT (Time table) are guaranteed to be 10bit max
- Values of LT (Length table) are guaranteed to be 12bit max
- Values of SVE table (the En value) are guaranteed to be 10bit max
- k is a 16 bit number
- all values and multiplications are unsigned integers

```

R1 = TT[TOF,E-index]; // 10 bit
R1 = R1 * LT[Ring,plate,sector,E-index]; // * 12 bit
R1 = R1 * SVE[E-index]; // * 10 bit // result is 32 bit
R1 = R1 >> 16; // result is 16 bit
R1 = R1 * Factor; // * 16 bit // result is 32 bit
R1 = R1 >> 16; // get index to MT table // result is 16 bit
if (R1 > 255) then R1 = 255; // R1 is used as index to MT
if (R1 == 0) then exit; // event is invalid.
M = MT[R1]/(128/n_M); // M is the mass group used for binning
    
```

3.6.2 Convert mass bin to atomic mass number

Given a mass group M in the data, the atomic mass m corresponding to it is retrieved as follows:

$$m^+ = M \cdot \text{floor}\left(\frac{128}{n_M}\right) \quad (3.28)$$

$$m^* = \begin{cases} m^+ \leq 63 & : m^+ \\ m^+ > 63 & : 3m^+ - 128 \end{cases} \quad (3.29)$$

$$\sqrt{m} = \frac{m^*}{\sqrt{512}} \quad (3.30)$$

The obtained mass does not include any energy loss because the loss is species and energy dependent. As a separate manual onground post-processing is needed to be done anyway for each species and energy, no onboard auto-correction has been done. The operation in Equation 3.29 requires also a correction of the histogram amplitudes:

$$C_{m^*} = \begin{cases} m^+ \leq 63 & : C_{m^+} \\ m^+ > 63 & : \frac{C_{m^+}}{3} \end{cases} \quad (3.31)$$

With C_{m^+} the amount of counts in the accumulation matrix at index m^+ and C_{m^*} the resulting amount of counts in the reconstructed accumulation matrix with 256 mass bins.

Abbreviations

CENA	Chandrayaan-1 Energetic Neutrals Analyzer
DPU	Digital Processing Unit
ESA	Electrostatic Analyzer
HV	High Voltage
MCP	Micro Channel Plate
SICD	Software Interface Control Document
SWIM	Solar Wind Monitor
TCTM	Telecommand/Telemetry (Control Document)
TOF	Time-Of-Flight